

REFINEMENT OF THE CRYSTAL STRUCTURE
OF SYNTHETIC PYROPEG. V. GIBBS¹ AND J. V. SMITH, *Department of the Geophysical
Sciences, University of Chicago, Chicago, Illinois*

ABSTRACT

Anisotropic least-squares analysis of synthetic pyrope yielded the distances: Si-O, 1.635; Al-O, 1.886; Mg-O, 2.198 and 2.343, all ± 0.002 Å. Shared oxygen-oxygen edges of polyhedra (2.496 for SiO₄ and MgO₆, and 2.618 for AlO₆ and MgO₆) are shorter than the unshared edges (2.753 in SiO₄, 2.716 in AlO₆ and 2.771, 2.783 in MgO₆, all ± 0.003 Å). The thermal vibration ellipsoid of the Mg atom is markedly anisotropic in conformity with the distorted nature of the MgO₆ polyhedron. A geometical analysis similar to that carried out by Born and Zemann shows that the steric details of the structure are consistent with a compromise between the attractive and repulsive ionic forces between both cations and anions.

INTRODUCTION

The crystal structure of the pyrope variety of garnet (Menzer, 1928) is of interest because of the complex interactions between the polyhedra, and because pyrope is stable only at elevated pressure as evinced both by its geological occurrence (see Tröger, 1959) and its laboratory synthesis (Coes, 1955; Boyd and England, 1959). We carried out an isotropic, three-dimensional, least-squares refinement of a crystal kindly supplied in 1957 by Dr. F. R. Boyd, Jr. of the Geophysical Laboratory from a sample grown at 1300° C. under 23 kilobars pressure. Before publication of our results, Zemann and Zemann (1961) described a careful, two-dimensional refinement of a synthetic pyrope crystal grown by Coes. Shortly thereafter expanded computer facilities permitted us to carry out an anisotropic, least-squares analysis of our three-dimensional data. About the same time, Zemann (1962) in a crystal-chemical study of garnet considered some of the factors governing the interatomic distances. He pointed out the elongation of the SiO₄ tetrahedron in both pyrope and grossular (whose structure has been refined by Abrahams and Geller (1958), and more recently by Prandl (1964)), and suggested that the concomitant shortening of the edge shared between the ZO₄ and XO₆ groups was to be expected from electrostatic considerations. It was also observed that the associated X-O bonds to the oxygen atoms comprising a shared edge were shorter than the other X-O bonds in violation of the expectation of a lengthening of the former because of cation-cation repulsion. Zemann then discussed the question of why there are no garnets with undistorted ZO₄ tetrahedra and YO₆ octahedra. Using reasonable Z-O and Y-O dis-

¹ Present address: Department of Geochemistry and Mineralogy, The Pennsylvania State University, University Park, Pennsylvania.

tances he found that regularity of the ZO_4 and YO_6 polyhedra demanded a short unshared edge (2.44 Å) in the XO_8 polyhedron, and concluded that the distortions of the tetrahedron and octahedron result from the need for unshared edges to be longer than 2.75 Å. More recently, Born and Zemann (1963; 1964) have published calculations on distances and lattice-energies of garnets. They found that the elongation and orientation of the tetrahedron could not be explained in terms of Coulomb attractive forces alone, and discovered that it was essential to include the repulsive forces between the oxygen anions and the divalent cations. To simplify the calculations, they assumed a fixed, distorted SiO_4 tetrahedron and a constant Al-O distance, and assigned a repulsive force of the type λd^{-n} to the oxygen atom and the divalent cation. Using a fully ionic model, only moderate agreement was obtained between the maximum of the partial lattice energy and the observed tetrahedral orientation, while assumption of partial ionization led to excellent agreement. The effect of tetrahedral distortion on the partial lattice energy was not so pronounced, but the observed distortion was favored in comparison to the ideal shape.

EXPERIMENTAL

A crystal showing {110}, {211}, {021} forms was ground to a polyhedron with maximum and minimum dimensions of 0.32 and 0.41 mm. Weissenberg and precession films exposed about the [100], [110] and [111] axes of the crystal possessed Laue and diffraction symmetry consistent with space group $Ia3d$. The intensities of 374 non-equivalent reflections (those within the CuK_α sphere of reflection) were measured from a scintillation-counter equi-inclination Weissenberg diffractometer using monochromatized MoK_α radiation. Absorption corrections were ignored because the use of penetrating MoK_α radiation reduced them to insignificance (about 1% in intensities). The polarizing effect of the bent quartz crystal monochromator also was about 1%, and was ignored.

The positional and isotropic temperature parameters determined by Zemann and Zemann (Table 1) were used as input in three cycles of isotropic least-squares refinement (Gibbs and Smith, 1962). The scattering curves used in the calculation were those of Berghuis *et al.* (1955) for Al^{3+} , Mg^{2+} , Si^{4+} and of Suzuki (1960) for O^{2-} , each modified arbitrarily for half-ionization, *i.e.*, $Al^{3+/2}$, Mg^+ , Si^{2+} and O^- . The calculations were made on an IBM 704 computer using the Busing-Levy program OR XLS (1959). Examination of the observed and calculated structure amplitudes for the strong low-angle reflections suggested that extinction effects were substantial. Consequently, five separate refinements were carried out, each of three cycles, using different weighting schemes. These calculations, made on an IBM 7090 computer using the Busing-Martin-Levy

TABLE 1. COMPARISON OF ATOMIC PARAMETERS FROM THREE REFINEMENTS

	Zemann and Zemann (1961)	Isotropic L.S. refinement of Zemann and Zemann data	Isotropic L.S. refinement Gibbs and Smith (1962)
x_0	0.034 (1)	0.0334 (5)	0.0329 (4)
y_0	0.050 (1)	0.0508 (5)	0.0508 (4)
z_0	0.654 (1)	0.6531 (5)	0.6531 (4)
B_0	0.4	0.37 (4)	0.38 (5)
B_{Mg}	0.3		0.67 (8)
B_{Al}	0.2	0.24	0.18 (5)
B_{Si}	0.3		0.13 (4)
Si-O	1.62	1.635 (6)	1.639 (5)
Al-O	1.89	1.888 (6)	1.887 (5)
Mg_1 -O	2.20	2.206 (6)	2.202 (5)
Mg_2 -O	2.35	2.337 (6)	2.335 (5)

The number in parentheses is the random experimental error. The refinement of the Gibbs and Smith data utilized all reflections equally weighted at unity.

program OR FLS (1962) for an anisotropic least-squares refinement, yielded the atomic parameters of Table 2. Refinement A used all observed reflections with unit weights; refinement B omitted the very strong 400 reflection; refinement C omitted all reflections with $|F_{obs}|$ greater than 200. For refinement D the unobserved reflections were added to those used in C and given an amplitude of zero. Three reflections 428, 206, and $6 \cdot 4 \cdot 10$ showed especially large discrepancies, and refinement E was made to test the effect of their omission on the atomic parameters. The parameters for D and E agree within the random experimental error, but those for the other refinements show discrepancies up to four times the random errors. The major changes result from omission of the 400 and other strong reflections, while the inclusion of the unobserved reflections produces changes, only one of which is greater than the random error. Because extinction seems to be the major factor in producing the differences, the atomic parameters from refinements A and B have been ignored. As there is no good reason to exclude reflections 428, 206, and $6 \cdot 4 \cdot 10$, refinement E has been discounted. Although some of the unobserved reflections have finite amplitudes, these are not known; consequently, the results from refinement D have been chosen in preference to those from C. The difference is so small that all conclusions drawn from these results are independent of this choice between refinements C and D. The random distribution of peaks in difference maps based on structure amplitudes for D confirmed the validity of the least-squares refinement. The difference maps were prepared with the IBM 1620 using the van der Helm three-

dimensional Fourier summation program (1961). The final R-factors are: all reflections, equally weighted 11.0%; observed reflections, equally weighted 8.5%; observed reflections excluding (400) 7.8%; observed reflections, excluded those with $|F| > 200$ 7.9%. Table 3 contains the observed and calculated structure amplitudes.

Because of discrepancies between the results obtained by Zemann and Zemann from F_0 and ΔF syntheses, and those obtained by us from least-squares methods, the structure amplitudes measured by Zemann and Zemann were submitted to isotropic least-squares refinement on the IBM 7074 using a modified version of the Busing-Martin-Levy program. As the silicon and magnesium atoms overlap in projection down z , it was necessary to ascribe arbitrarily fixed temperature factors to these atoms. The values 0.3 given by Zemann were chosen. Only those reflections listed by Zemann and Zemann as being unaffected by extinction, and as not being too weak, were used in the refinement. Table 1 shows agreement within the error limits for the parameters from the new refinement of the Zemann-Zemann data and the original refinement of the Gibbs-Smith data. Thus the two sets of data are consistent and there is no need to suppose that there is any structural difference between the two synthetic specimens. The random arrangement of peaks in the difference synthesis calculated from the data of our isotropic refinement suggests that refinement by difference syntheses would have led to essentially the same

TABLE 2. ATOMIC PARAMETERS FROM DIFFERENT REFINEMENTS

	A	B	C	D	E
<i>Oxygen</i>					
x	0.03386 (32) ¹	0.03291 (23)	0.03275 (18)	0.03284 (19)	0.03285 (17)
y	.05091 (28)	.04990 (21)	.05002 (17)	.05014 (18)	.05013 (16)
z	.65282 (28)	.65328 (21)	.65329 (16)	.65330 (18)	.65327 (16)
β_{11}	.00093 (16)	.00094 (12)	.00091 (09)	.00099 (10)	.00103 (09)
β_{22}	.00073 (15)	.00085 (11)	.00101 (09)	.00103 (10)	.00110 (09)
β_{33}	.00046 (14)	.00069 (11)	.00070 (08)	.00078 (09)	.00085 (09)
β_{12}	.00032 (13)	.00024 (09)	.00016 (07)	.00013 (08)	.00011 (07)
β_{13}	.00001 (12)	-.00001 (09)	-.00006 (07)	-.00014 (07)	-.00017 (06)
β_{23}	-.00007 (12)	-.00002 (09)	-.00010 (07)	-.00009 (07)	-.00006 (06)
<i>Aluminum</i>					
β_{11}	.00035 (06)	.00051 (05)	.00058 (04)	.00060 (04)	.00064 (04)
β_{12}	.00005 (09)	.00002 (06)	.00002 (05)	.00004 (05)	.00003 (04)
<i>Magnesium</i>					
β_{11}	.00050 (19)	.00086 (15)	.00095 (12)	.00102 (13)	.00104 (11)
β_{22}	.00148 (14)	.00159 (11)	.00171 (09)	.00167 (09)	.00165 (08)
β_{23}	.00037 (20)	.00041 (15)	.00045 (12)	.00041 (12)	.00042 (10)
<i>Silicon</i>					
β_{11}	.00034 (12)	.00053 (09)	.00057 (07)	.00056 (08)	.00059 (07)
β_{12}	.00026 (07)	.00039 (05)	.00045 (04)	.00046 (05)	.00050 (04)

¹ The number in parentheses is the random experimental error.

Table 3.

Observed and calculated structure amplitudes for pyrope

hkl	F _o	F _c	hkl	F _o	F _c	hkl	F _o	F _c	hkl	F _o	F _c
400	255	356	9.3.12	21	22	9.3.16	23	24	14.3.19		2
214	36	33	4.4.12	97	-94	11.3.16	7	-8	16.3.19		0
202	33	32	6.4.12	15	-15	13.1.16	6	7	7.4.19	24	19
213	38	-41	8.4.12	21	-19	6.4.16	77	87	9.4.19	30	31
233	174	-172	7.5.12	7	7	8.4.16	85	85	11.4.19	12	-9
633			6.6.12	119	120	10.4.16	40	39	13.4.19		6
204	241	-269	4.1.13	-1	-1	12.4.16	10	10	15.4.19	10	12
404	82	-82	6.1.13	30	-29	7.5.16	20	-20	6.5.19	21	17
224	142	139	8.1.13	22	21	9.5.16	10	10	8.5.19	4	7
844	41	44	10.1.13	0	0	11.5.16	4	7	10.5.19		-2
215	81	-84	12.1.13	7	-4	6.6.16	18	19	12.5.19	20	-22
415	22	19	3.2.13	2	2	8.6.16	7	6	14.5.19	16	14
325	79	73	5.2.13	76	67	10.6.16	10	11	7.6.19	26	22
206	124	108	7.2.13	4	4	9.7.16	0	0	9.6.19	4	-7
406	282	312	9.2.13	19	21	8.8.16	135	145	11.6.19	18	20
606	6	-3	11.2.13	5	5	8.1.17	15	-12	13.6.19		2
116	149	137	4.3.13	22	-22	10.1.17	15	6	8.7.19	27	-23
316	44	-44	6.3.13	37	-37	12.1.17	18	-18	10.7.19	10	-3
516	2	-2	8.3.13	34	31	14.1.17	7	7	12.7.19	14	15
426	284	288	10.3.13	14	14	16.1.17	3	3	9.8.19	27	30
217	18	-17	7.4.13	19	22	7.2.17	11	-9	11.8.19	14	-15
417	66	64	7.4.13	15	15	9.2.17	16	16	10.9.19		-9
617	86	84	9.4.13	13	14	11.2.17	22	-23	12.0.20	22	-20
327	64	-63	6.5.13	3	3	13.2.17	19	-13	14.0.20	32	-27
527	58	57	8.5.13	32	-33	15.2.17	-3	-3	16.0.20	16	17
437	34	-36	7.6.13	14	13	6.3.17	-8	-8	18.0.20	21	19
208	59	52	6.0.14	17	-17	8.3.17	21	19	13.1.20	3	3
408	246	227	8.0.14	35	29	10.3.17	1	1	15.1.20	-5	-5
608	12	-12	10.0.14	33	33	12.3.17	19	-20	17.1.20	10	-14
808	351	335	12.0.14	92	95	14.3.17	22	-24	19.2.20	38	34
318	13	-13	14.0.14	16	-13	5.4.17	32	-28	12.2.20	12	6
518	58	66	5.1.14	61	-52	7.4.17	27	-23	14.2.20	45	41
718	19	-18	7.1.14	2	4	9.4.17	28	-24	16.2.20	10	8
228	42	-41	9.1.14	22	-23	11.4.17	2	2	9.3.20		-3
428	166	-190	11.1.14	9	-4	13.4.17	-4	-4	11.3.20	-3	-3
628	22	-21	13.1.14	-4	-4	6.5.17	55	-48	13.3.20	13	10
538	86	-92	4.2.14	172	159	8.5.17	3	9	15.3.20	4	4
219	14	14	6.2.14	15	15	10.5.17	-3	-3	8.4.20	11	-8
419	92	91	8.2.14	23	-16	12.5.17	6	-6	10.4.20	49	-16
619	5	0	10.2.14	13	10	7.6.17	-3	-3	12.2.20	47	-47
819	44	44	12.2.14	54	49	9.6.17	-4	-4	16.4.20	6	6
329	11	8	5.3.14	4	4	11.6.17	20	-18	7.5.20	12	-12
529	21	21	7.3.14	9	7	8.7.17	13	13	11.5.20		-6
729	36	-38	9.3.14	9	9	10.7.17	15	15	13.5.20	3	3
439	46	-44	11.3.14	33	35	9.8.17	-4	-4	15.5.20	9	9
639		-3	6.4.14	95	94	10.0.18	14	10	8.6.20	60	64
849	10	-10	8.4.14	99	-101	12.0.18	98	90	10.6.20	50	46
2.0.10	98	-94	10.4.14	72	73	14.0.18	-7	-7	12.6.20	20	22
4.0.10	225	197	12.4.14	42	-38	16.0.18	12	-15	14.6.20	42	42
6.0.10	46	-43	7.5.14	14	-16	18.0.18	13	-13	9.7.20	8	8
8.0.10	14	-14	9.5.14	3	3	9.1.18	14	11	11.7.20	9	13
10.0.10	97	105	8.6.14	14	17	11.1.18	15	14	13.7.20	5	5
3.1.10	12	15	7.7.14	28	-28	13.1.18	-7	-7	15.7.20	53	54
5.1.10	9	-8	6.1.15	30	29	15.1.18	20	24	10.8.20	34	-35
7.1.10	16	-17	8.1.15	47	44	17.1.18	-3	-3	12.8.20	14	13
9.1.10	13	14	10.1.15	2	2	8.2.18	1	1	11.9.20		-2
4.2.10	194	194	12.1.15	13	-11	10.2.18	28	-28	12.1.21	9	10
6.2.10	37	-39	14.1.15	25	23	12.2.18	61	58	16.1.21		2
8.2.10	23	17	5.2.15	20	22	14.2.18	13	7	11.2.21	12	-15
3.3.10	7	6	7.2.15	-5	-5	16.2.18	6	6	15.2.21	16	-14
5.3.10	3	2	9.2.15	30	29	7.3.18	12	7	17.2.21	11	11
7.3.10		-6	11.2.15	37	-39	9.3.18	19	-15	10.3.21	13	15
6.4.10	123	141	13.2.15	15	15	11.3.18	8	-8	14.3.21	20	-21
5.5.10	17	19	4.3.15	8	12	13.3.18	17	-17	9.4.21	13	10
2.1.11	2	2	6.3.15	4	4	15.3.18	31	-33	11.4.21	15	-12
4.1.11	43	-41	8.3.15	15	14	6.4.18	77	72	13.4.21	19	20
6.1.11	26	26	10.3.15	10	-11	8.4.18	66	-72	8.5.21	4	4
8.1.11	30	-27	12.3.15	8	6	10.4.18	56	53	12.5.21	16	15
10.1.11	13	-16	5.4.15	27	-26	12.4.18	-7	-7	7.6.21	34	35
3.2.11	24	-21	7.4.15	3	-6	14.4.18	57	58	11.6.21	11	10
5.2.11	35	34	9.4.15	21	-21	7.5.18	-6	-6	13.6.21	24	-27
7.2.11	4	4	11.4.15	42	3	9.5.18	3	3	15.6.21	18	17
9.2.11	8	9	6.5.15	25	24	11.5.18	-2	-2	9.8.21	17	18
4.3.11	18	-16	8.5.15	29	26	13.5.18	24	-24	13.8.21		6
6.3.11	47	-46	10.5.15	10	-12	8.6.18	13	12	10.9.21	7	4
8.3.11	25	-23	7.6.15	11	-10	10.6.18	16	17	12.9.21	11	-15
5.4.11		-1	9.6.15	5	-6	12.6.18	58	59	11.10.21	8	-6
7.4.11	59	-54	8.7.15	20	-19	7.7.18	16	-16	16.0.22	10	7
6.5.11	10	8	8.0.16	199	201	9.7.18	0	0	13.1.22	15	12
4.0.12	33	32	10.0.16	10	-11	11.7.18	20	-21	11.3.22	15	16
6.0.12	115	-113	12.0.16	108	99	10.8.18			13.3.22	18	16
8.0.12	124	124	14.0.16	36	33	12.8.18	27	34	15.3.22	11	12
10.0.12	95	-90	16.0.16	123	117	10.1.19	26	-27	10.4.22	60	50
12.0.12	9	-7	7.1.16	16	-19	12.1.19	-2	-2	14.4.22	52	52
3.1.12	43	38	9.1.16	17	20	14.1.19	16	14	11.5.22	18	-15
5.1.12	6	6	11.1.16	6	6	16.1.19	2	2	8.6.22	6	7
7.1.12	5	5	13.1.16	0	1	18.1.19	4	4	12.6.22	37	40
9.1.12	17	-17	15.1.16	12	-9	9.2.19	23	19	9.7.22	4	-2
11.1.12	43	-38	6.2.16	12	-9	11.2.19	10	-9	13.7.22	14	18
4.2.12		5	8.2.16	20	-17	13.2.19	13	13	11.4.23	13	-15
6.2.12	113	107	10.2.16	28	29	15.2.19	15	-14	13.4.23	20	-19
8.2.12	114	125	12.2.16	67	-66	17.2.19	-1	-1	12.5.23	10	7
10.2.12	118	117	14.2.16	21	14	8.3.19	12	-12	11.8.23	18	-20
5.3.12	25	33	5.3.16	14	10	10.3.19	17	-17	12.4.24	9	12
7.3.12	46	-43	7.3.16	22	-24	12.3.19		-2			

coordinates as those obtained from the anisotropic least-squares refinement.

The cell edge 11.459 Å found by Skinner (1956) for a synthetic pyrope was used in the calculations of interatomic distances and angles (Table 4). The estimated standard deviations, obtained in the final least-squares calculation, are given in parentheses in Table 2. For the D refinement these lead to standard deviations 0.002 Å for Al-O, Mg-O and Si-O and 0.003 Å for O-O. The final anisotropic temperature factors β_{ij} obtained from the refinement are also listed in Table 2. Certain constraints exist among the temperature factors of the atoms in special positions, *i.e.*, for magnesium, $\beta_{11} \neq \beta_{22} = \beta_{33}$ and $\beta_{12} = \beta_{13} = \beta_{23}$ and for aluminum and silicon, $\beta_{11} = \beta_{22} = \beta_{33}$ and $\beta_{12} = \beta_{13} = \beta_{23} = 0$. The three principal axes of the thermal vibration ellipsoid for each atom were computed using the Busing-

TABLE 4. INTERATOMIC DISTANCES¹ AND ANGLES IN PYROPE

SiO ₄ tetrahedron	Si-O	(4) ²	1.635 Å
	O-O	(2)	2.496, (4) 2.753
	O-Si-O	(2)	99.6°(2) 114.7
AlO ₆ octahedron	Al-O	(6)	1.886 Å
	O-O	(6)	2.618, (6) 2.716
	O-Al-O	(6)	87.9° (6) 92.1
MgO ₃ cube	Mg ₁ -O	(4)	2.198 Å
	Mg ₂ -O	(4)	2.343
	O-O	(2)	2.496, (4) 2.618
		(4)	2.711, (2) 2.783
	O-Mg ₁ -O	(2)	69.2°
	O-Mg ₂ -O	(2)	72.9°, (2) 109.4
	O-O-O	(4)	76, (2) 79, (2) 88
		(4)	92, (2) 94, (2) 94
		(2)	101, (2) 103, (2) 112
		(2)	119
	Mg-Al	(4)	3.203 Å
	Mg-Si	(2)	2.865, (4) 3.509
	Al-Si	(6)	3.203
	Si-O-Al	130°	
	Si-O-Mg ₁	95	
Si-O-Mg ₂	123		
Mg ₁ -O-Mg ₂	101		
Al-O-Mg ₁	103		
Al-O-Mg ₂	98		

¹ These distances are not corrected for atomic motions; the corrections are small because of the low temperature factors. (See Busing and Levy, 1964.)

² The number in parentheses is the frequency of occurrence.

TABLE 5. THE R.M.S. DISPLACEMENTS AND ORIENTATIONS OF THE PRINCIPAL AXES OF THE THERMAL VIBRATION ELLIPSOIDS

Atom	r	u(r)	$\theta(r, x)$	$\theta(r, y)$	$\theta(r, z)$
O	1	0.0708 (36) Å	58.8 (12.3) ⁰	89.6 (13.4)	31.2 (12.2)
	2	0.0807 (36)	56.8 (15.0)	140.5 (14.1)	108.9 (16.1)
	3	0.0913 (33)	48.9 (11.7)	50.4 (14.1)	113.8 (8.7)
Al	1	0.0633 (32)	1	1	1
	2	0.0633 (31)	1	1	1
	3	0.0693 (47)	54.7	54.7	54.7
Mg	1	0.0832 (46)	0.0	90.0	90.0
	2	0.0915 (44)	90.0	45.0	135.0
	3	0.1171 (41)	90.0	45.0	45.0
Si	1	0.0573 (21)	1	1	1
	2	0.0573 (36)	1	1	1
	3	0.0627 (36)	0.0	90.0	90.0

¹ Indeterminate (uniaxial thermal ellipsoid).

r_1, r_2, r_3 are the ellipsoid axes, and x, y, z the crystallographic axes.
The experimental errors are enclosed in parentheses.

Martin-Levy OR FFE program (1964). The r.m.s. displacements and their orientations with respect to the crystallographic axes are given in Table 5.

DISCUSSION

The structure of pyrope consists of independent SiO_4 and AlO_6 polyhedra (Fig. 1) which share corners to form an aluminosilicate framework within which each magnesium atom is surrounded by an irregular polyhedron of eight oxygen atoms (Figs. 2, 3). The sharing coefficients of the SiO_4 and AlO_6 polyhedra are one compared with two for the MgO_8 polyhedron (Zoltai, unpublished). Accordingly, each oxygen atom is coordinated by a silicon atom at 1.635 Å, by an aluminum atom at 1.886 Å and by two magnesium atoms at 2.198 and 2.343 Å (Fig. 3). Zemann (1962) has suggested that the polyhedron about the magnesium atom is best regarded as a distorted cube. Two edges of the silicon tetrahedron and six edges of the aluminum octahedron are shared with the magnesium cube leaving unshared four edges in the tetrahedron, six in the octahedron and six in the cube. In fact, the high density and high refractive indices of pyrope, and of garnet in general, can be attributed to the large percentage of shared edges which leads to a tightly packed arrangement.

The shared edges are shorter than the unshared edges:

shared between SiO_4 and MgO_8	2.496 Å;
shared between AlO_6 and MgO_8	2.618;
unshared SiO_4	2.753;
unshared AlO_6	2.716;
unshared MgO_8	2.711, 2.783.

This leads to considerable distortion of the polyhedra. The silicon tetrahedron is a tetragonal bispphenoid elongated along the $\bar{4}$ axis while the

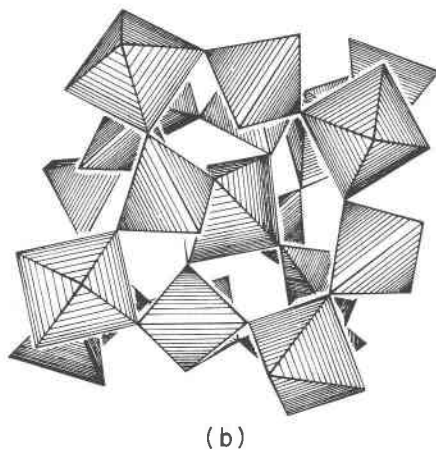
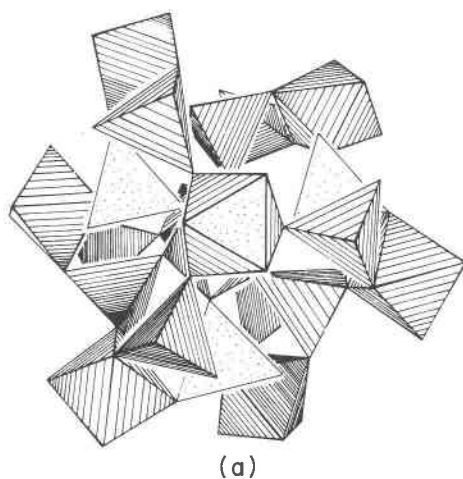


FIG. 1. Idealized drawings of the SiO_4 and AlO_6 polyhedra in pyrope viewed down $\bar{3}$ (a) and along z (b); the MgO_8 polyhedra have been omitted for clarity and the polyhedra have been displaced slightly to avoid superposition.

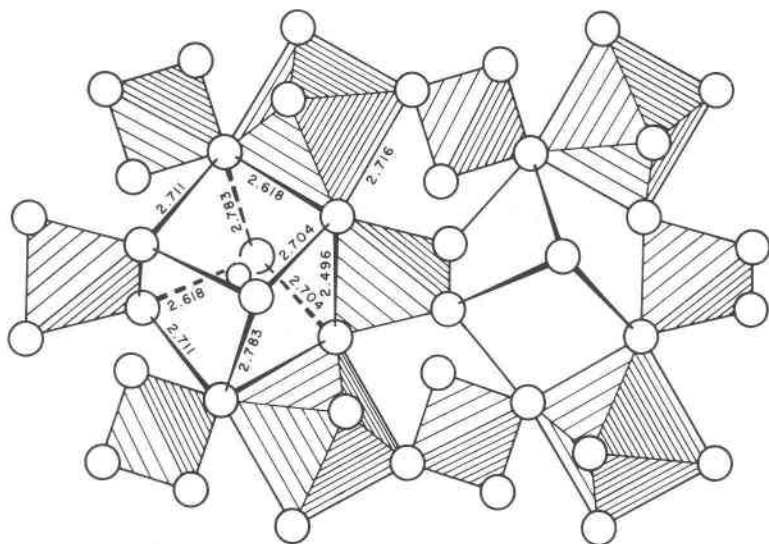


FIG. 2. Part of the pyrope structure projected down the z -axis. The large open circles represent oxygen atoms and the smaller one within the open cube is magnesium. Aluminum and silicon atoms center the octahedra and tetrahedra, respectively, and a magnesium atom centers the closed cube; these are not indicated. The values along the edges of the polyhedra refer to O-O distances.

aluminum octahedron is a trigonal antiprism elongated along the $\bar{3}$ axis. The Mg cube is considerably distorted with its plane angles varying from 76 to 119°.

It might be expected that the thermal vibration ellipsoid of a cation would depend on the distortion of its coordination polyhedron of anions. Indeed, the orientation and the anisotropy of the thermal ellipsoid of the magnesium atom in pyrope conform to the distorted nature of its coordination polyhedron. Figure 4(a) is a stereographic projection of the neighbors of the magnesium atom and the axes of the thermal ellipsoid.¹ The shortest axis (r.m.s. displacement 0.0832 (46) Å) bisects the two shorter Mg₁-O bonds (2.198 Å) which make an angle of 69° with one another. The intermediate axis (0.0915 (44)) bisects two of the longer Mg₂-O bonds (2.343 Å) which make an angle of 73°, while the longest axis (0.1171 (41)) also bisects longer bonds but at an angle of 109°. It is of interest that the longest axes of the thermal ellipsoids for the silicon

¹ Zemann and Zemann (1962) tentatively suggested slight disorder of the Mg atom to explain anisotropy of the electron density, and approximated the disorder by a statistical distribution over the general position (0.125, 0.003, 0.253). This anisotropy is in the same direction as that found by anisotropic least-squares refinement.

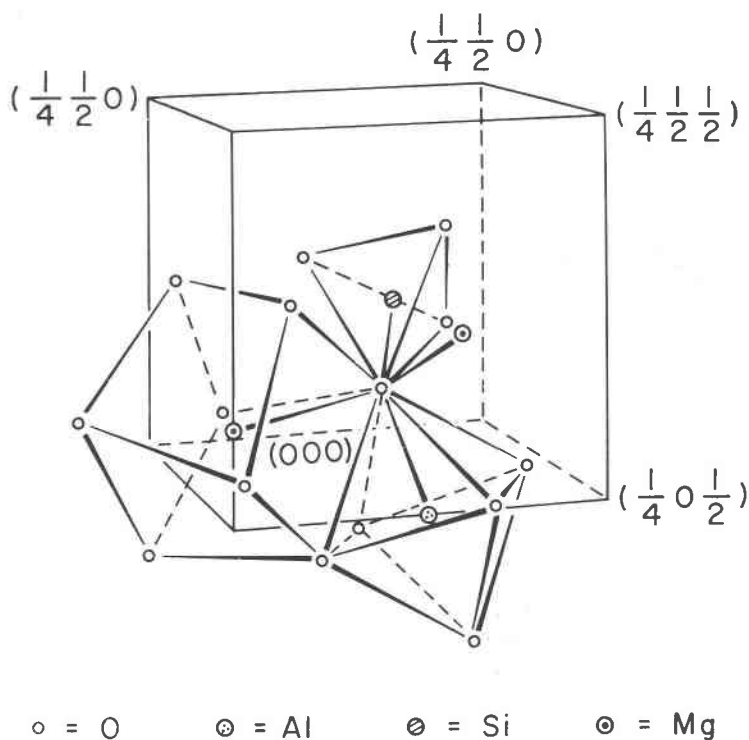


FIG. 3. The coordination polyhedra of oxygen atoms about Al, Mg and Si in pyrope; one of the cubes about Mg is omitted (Modified after Abrahams and Geller, 1958).

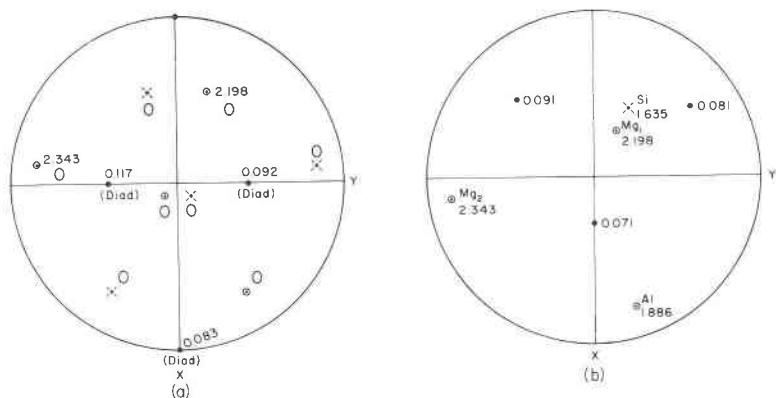


FIG. 4. Stereograms of the first coordination spheres and the thermal vibration ellipsoid axes of the Mg-atom (a) and the oxygen atom (b). The values of the r.m.s. displacements and the bond lengths are in Å. The principal axes of the vibration ellipsoids are represented by solid dots; the crossed and encircled dots represent cyclographic projections of bonds to first co-ordination sphere atoms lying above and below the primitive, respectively.

and aluminum atoms are also oriented in conformity with the distortions of their polyhedra; however, the ellipsoids are not significantly anisotropic as the axes differ only by about 1σ (r.m.s. displacements and random errors are: Si 0.0573 (21), 0.0573 (36) and 0.0627 (36); Al 0.0633 (32), 0.0633 (31) and 0.0693 (47) Å). Figure 4(b) shows the relation between the thermal ellipsoid and environment of the oxygen atom. The anisotropy is statistically significant, but no interpretation is offered. Experimental values of thermal vibration ellipsoids necessarily combine positional disorder and true thermal vibration. The ellipsoids for Si, Al and O are similar in size to those for olivine (Gibbs *et al.*, 1964) and aluminosilicates (Burnham and Buerger, 1961; Burnham, 1962; Burnham, 1963) and it seems likely that all of them result only from true thermal vibration. The ellipsoid for Mg, however, is larger than might be expected; indeed, it is significantly larger than that of the oxygen atom. It is suggested that conflicting spatial requirements result in the magnesium atom lying in a cavity larger than normal, and that it tends to fill the cavity by a strong asymmetric vibration. Because there are no optical or x-ray anomalies from isometric symmetry, it is likely that if there are potential energy minima, the Mg atoms occupy these at random.

Miyashiro (1953) has suggested that in the pyrospite garnets (*i.e.* those with a small atom in the eight-coordinated site) four of the eight oxygen atoms will be closer to the eight-coordinated atom tending to approach the lower coordination number more commonly found for magnesium and the other small cations. Indeed the magnesium atom in pyrope does have four close neighbors at 2.198 and four more distant ones at 2.343 Å. However, this feature is found in all garnets so far investigated (grossular (Abrahams and Geller, 1958; Prandl, 1964), $Y_3Fe_2Fe_3O_{12}$ (Geller and Gilleo, 1957; Batt and Post, 1962), $Gd_3Fe_2Fe_3O_{12}$ (Weidenborner, 1961), $Y_3Al_2Al_3O_{12}$ (Prince, 1957), hydrogarnet (Cohen-Addad *et al.*, 1963) and appears to be a general property of the garnet structure rather than a feature unique to cations which normally have a lower coordination number. For example, calcium tends to have a coordination number between 6 and 9 but it still has four near oxygen neighbors in both grossular and hydrogarnet.

In a similar manner to Zemann (1962) and Born and Zemann (1964), we have attempted to understand the structure of pyrope in terms of ionic bonding, following the classical treatment described most recently by Pauling (1960). The basic conclusions are similar to those of Born and Zemann, but there are some differences in emphasis which we feel are important.

The Si-O bond is strong and its length almost immune to change by the neighboring cations. Smith and Bailey (1963) have shown that the mean Si-O distance in a tetrahedron varies from 1.61 Å for a tektosilicate to

1.63 Å for structures with isolated tetrahedra. Within each group of silicates, the observed values fall within a range of about 0.01 Å. The Si-O bond length in pyrope, 1.635 Å, is in excellent agreement with values recorded for other nesosilicates which have tetrahedra sharing one or more edges with other polyhedra: for example, fayalite 1.632 (Hanke, 1964), spurrite 1.633 (Smith, *et al.*, 1960), forsterite 1.634, hortonolite 1.638 (Gibbs, *et al.*, in preparation) and grossular 1.637 Å (Abrahams and Geller, 1958). These values are somewhat longer than the value 1.628 Å found in the nesosilicates andalusite (Burnham and Buerger, 1961) and kyanite (Burnham, 1963), whose tetrahedra do not share edges with the other polyhedra. It appears that the longer distances in the former are induced by repulsive forces between cations over a shared edge (Pauling, 1928). (Indeed the variation of Si-O distance from 1.61 Å in a tectosilicate to 1.63 Å in a nesosilicate may result in part from repulsion between two silicon atoms sharing a common oxygen atom.) Thus it seems reasonable to expect for all garnet structures an Si-O distance within 0.005 Å of 1.635 Å.

The Al-O distance in the trigonal antiprism, 1.886 Å, is shorter than the mean values recorded for a number of other silicates: synthetic beryl 1.898 (Gibbs and Breck, in preparation), euclase 1.90 (Mrose and Appleman, 1962), kyanite 1.906 (Burnham, 1963), mullite 1.911 (Burnham, 1964), paragonite 1.912 and muscovite 1.916 (Burnham and Radoslovich, 1964), jadeite 1.927 (Prewitt and Burnham, 1964), andalusite 1.934 (Burnham and Buerger, 1961) and grossular 1.945 Å (Abrahams and Geller, 1958). Because the Al-O octahedral bond is weaker than the Si-O tetrahedral bond, the influence of neighbors should be greater, and a larger spread of Al-O distances is to be anticipated. The range from 1.886 in pyrope to 1.945 Å in grossular is rather large, and indicates that the Al-O distance is being affected seriously by neighboring atoms.

The Mg-O bond is relatively weak because of the lower charge of the cation and the higher coordination number. The wide spread of Ca-O, Na-O and K-O distances is well-known, and requires no detailed documentation. For grossular, the difference of 0.16 Å between the two Ca-O distances in the XO_8 group is in line with the variation in other silicates. By analogy it seems reasonable to expect a difference of at least 0.1 Å between the two Mg-O distances, and the observed difference of 0.13 Å in pyrope need cause no surprise.

Cation-cation repulsion should be strongest across the shared edge between the SiO_4 and MgO_8 polyhedra. The observed values of 2.50 and 2.62 Å, respectively, for the shared edges joining MgO_8 to the SiO_4 and AlO_6 polyhedra are reasonable when compared with the distortions of the octahedra in corundum (Newnham and deHaan, 1962) and the TiO_2

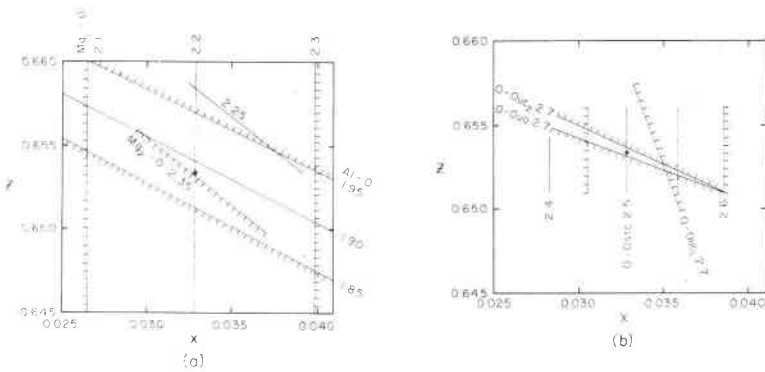


FIG. 5. Plot of x vs. z positional parameters of the oxygen atom in pyrope, for selected interatomic distances: (a) Mg₁-O, Mg₂-O, Al-O; (b) O-O: O-O_{STC} refers to shared edge between SiO₄ and MgO₈ polyhedra; O-O_{UC}, the unshared edge of the AlO₆ polyhedron and O-O_{UC} the unshared edge of the MgO₈ polyhedron. Hatched lines indicate limits of reasonable variation of interatomic distances.

polymorphs (Pauling, 1960). The corresponding values in grossular, 2.56 and 2.79 Å, are larger in conformity with the longer Ca-Si and Ca-Al distances, and consequent lower repulsion. However, in grossular the unshared edge of the AlO₆ polyhedron is shorter than the shared edge (2.71 Å) indicating that the distortion of the octahedron is not determined entirely by cation-cation repulsion.

The lengths of the unshared edges of the polyhedra should depend primarily on the cation and the lengths of the shared edges. The mean cation-oxygen distance is determined primarily by the cation; if the shared edges are shortened by cation-cation repulsion, those remaining should be lengthened in order to preserve the mean value required by a constant cation-oxygen distance.

Although a crystal structure will not be stable unless all the spatial requirements are satisfied, it would be remarkable if all the requirements were satisfied exactly. Some compromise can be expected in all complex structures, with the amount of compromise for each requirement being determined by the nature of the bonding forces. In order to see the interaction between the interatomic distances, we have prepared Fig. 5 which is a graph of the interatomic distances as a function of the x and z coordinates of the oxygen atom. The third coordinate, y , was determined by assuming that Si-O = 1.635 Å and that $a = 11.459$ Å. Born and Zemann have prepared similar graphs on the assumption that Si-O = 1.62 Å, Al-O = 1.89 Å and a is variable. From Fig. 5(a) it may be seen that for pyrope there is a strong interaction between the Al-O and Mg-O distances. For an Mg₁-O distance between 2.1 and 2.3 Å, which may be re-

garded as reasonable outer limits for a magnesium atom in eight-fold coordination, and for Al-O distances less than 1.95 Å, a reasonable upper limit for an aluminum atom in six-fold coordination, the Mg₂-O distance must be greater than 2.24 Å. If the average of the two Mg-O distances is to lie between 2.2 and 2.25 Å while the Al-O distance is close to 1.90 Å, the coordinates of the oxygen atom can vary only between narrow limits. Figure 5(b) shows the effect on the O-O distances as the oxygen atom moves. The control exerted by the unshared polyhedral edges is remarkable, a conclusion already reached by Zemann (1962). Only three of the unshared edges are plotted because the one in the tetrahedron changes only from 2.7 to 2.8 Å over the entire range of Fig. 5 (all three have been assumed to be not shorter than 2.7 Å). The edge shared between the octahedron and cube varies only from 2.55 to 2.73 Å over the entire range of Fig. 5 and was not plotted because all these values are possible if a tolerance of about 0.1 Å is permitted. The edge shared between the tetrahedron and cube should be shortened considerably and a value near 2.5 Å appears reasonable. If a rather wide range from 2.45 to 2.6 Å is permitted, about half of the area of Fig. 5(b) is permissible for this shared edge. When all the spatial considerations for the oxygen atoms are combined together, only a small area is permitted in Fig. 5(b), and indeed the observed position of the oxygen atom is at the center of this region. Returning to Fig. 5(a) it will be seen that the small area of Fig. 5(b) is consistent with the larger area permitted for the Mg-O and Al-O bonds, and that application of the limits of the oxygen co-ordinates deduced from the oxygen atoms results in very restricted ranges for the Mg-O and Al-O distances. Zemann (1962) pointed out that cation-cation repulsion should cause the Mg₁-O distance to the oxygen atoms forming a shared edge with the silicon tetrahedron to be longer than the Mg₂-O distance. Actually it is shorter, and Zemann concluded that this resulted from the need for unshared oxygen edges to be longer than 2.75 Å. (Theoretically cation-cation distances can increase without change in cation-anion distances if the anion-anion shared edges are shortened). From Fig. 5 it can be seen that if Mg₁-O is longer than Mg₂-O quite unreasonable values are produced for both O-O unshared edges and for Al-O. As high coordination, low-charge cations show large variations of distances to neighboring anions, the inequality of the two Mg-O distances is not surprising because the mean value of 2.2 Å is quite reasonable.

CONCLUSION

A similar analysis of the crystal structure can be carried out for any garnet, and indeed it seems likely that such a method will yield an excellent prediction of the coordinates of the oxygen atom. In order to test

this and other structural features we are preparing least-squares anisotropic refinements for almandine and other garnets. It is remarkable how closely the competing spatial factors can be satisfied over such wide ranges of chemical composition in a structure with such high symmetry and few variable atomic parameters. The deviations of observed distances from those to be expected from consideration of just the first and second neighbors amount only to 0.1 Å for the weaker bonds, and are much less for the stronger bonds. The general principle that all bonds must be satisfied within these tolerances, and that the finer details are determined by a compromise between the attractive and repulsive forces of both cations and anions, hopefully applies to other complexly-bonded structures such as aluminosilicates and olivine. However, analyses of these minerals will be more difficult, and perhaps impossible, because of the lower symmetry and larger number of variable parameters. Born (1964) has presented a lattice-energy calculation of olivine which gives a good prediction of the position of the oxygen atom. Although covalent bonding presumably plays an important role in the garnet structure, the success of the above treatment based solely on ionic bonding supports the statement of Verhoogen (1958) that silicates of magnesium and aluminum behave mostly as purely ionic compounds.

ACKNOWLEDGMENTS

The authors wish to thank Dr. Francis R. Boyd, Jr., of the Geophysical Laboratory, Washington, D.C. for donating the crystal used in the study, Mr. Charles Knowles for aid in the collection and correction of the data; Dr. Charles W. Burnham of the Geophysical Laboratory, Dr. Charles T. Prewitt of the E. I. Du Pont de Nemours Central Research Department, Professor Adolf Pabst of the Geology and Geophysics Department at the University of California, and Dr. Earle R. Ryba of the Metallurgy Department at The Pennsylvania State University for critically reading the paper; Dr. Chester M. Smith of the Computation Center at The Pennsylvania State University for assistance in modifying the Busing-Martin-Levy Least Squares Program for the IBM 7074; and the National Science Foundation for grants G-14467 and GP-443 which supported this research. Professor J. Zemann has assisted us considerably by correspondence.

REFERENCES

- ABRAHAMS, S. C. AND S. GELLER (1958) Refinement of the structure of a grossularite garnet. *Acta Cryst.* 11, 437-441.
BATT, A. AND B. POST (1962) A procedure for parameter refinement in simple structures. *Acta Cryst.* 15, 1268-1270.
BERGHUIS, J., I. HAANAPPEL, M. POTTERS, B. LOOPSTRA, C. MACGILLAVRY AND

- A. VEENENDAAL (1955) New calculations of atomic scattering factors. *Acta. Cryst.* **8**, 478-483.
- BORN, L. (1964) Eine "gitterenergetische Verfeinerung" der freien Mg-position in Olivin. *Neues. Jb. Mineral. Mh.* **3**, 81-94.
- AND J. ZEMANN (1963) Gitterenergetische Berechnungen an Tonerdegranaten. *Acta. Cryst.* **16**, 1064-1065.
- AND J. ZEMANN (1964) Abstandsberechnungen and gitterenergetische Berechnungen an Granaten. *Beit. Mineral. Petr.* **10**, 2-23.
- BOYD, F. R. AND J. L. ENGLAND (1959) Pyrope. *Ann. Rept. Director Geophys. Lab.* **1320**, 83-87.
- BURNHAM, C. W. (1963) Refinement of the crystal structure of kyanite. *Zeit. Kristal.* **118**, 337-360.
- (1964) Crystal structure of mullite. *Carnegie Inst. Washington Yearbook*, **63**, 1440, 226.
- AND M. J. BUERGER (1961) Refinement of the crystal structure of andalusite. *Zeit. Kristal.* **115**, 269-290.
- AND E. W. RADOSLOVICH (1964) Crystal structures of coexisting muscovite and paragonite. *Carnegie Inst. Washington Yearbook* **63**, 1440, 232-238.
- BUSING, W. R. AND H. A. LEVY (1959) A crystallographic least-squares refinement program for the IBM 704 ORNL, Oak Ridge, Tenn.
- AND H. A. LEVY (1964) The effect of thermal motion on estimation of bond lengths from diffraction measurements. *Acta. Cryst.* **17**, 142-146.
- , K. O. MARTIN, AND H. A. LEVY (1962) ORFLS, A Fortran crystallographic least-squares program. ORNL, Oak Ridge, Tenn.
- , K. O. MARTIN, AND H. A. LEVY (1964) ORFFE, A Fortran crystallographic function and error program. ORNL, Oak Ridge, Tenn.
- COES, L. (1955) High-pressure minerals. *Am. Ceram. Soc.* **38**, 298.
- COHEN-ADDAD, P. DUCROS, DURIF-VARAMBON, E. F. BERTAUT AND A. DALAPALME (1963) Etude de la position des atomes d'hydrogene dans l'hydrogrenat Al_2O_3 , $3CaO$, $6H_2O$. *Solid State Comm.*, **1**(4), 85-87.
- GELLER, S. AND M. A. GILLES (1957) The crystal structure and ferro-magnetism of yttrium-iron garnet $Y_3Fe_2(FeO_4)_3$. *Jour. Phys. Chem. Solids* **3**, 30-36.
- GIBBS, G. V., P. B. MOORE, AND J. V. SMITH (1964) Refinement of the crystal structures of forsterite and hortonolite (in preparation).
- AND J. V. SMITH (1962) Crystal structure of pyrope (abs.) *1962 Ann. Meet. Geol. Soc. Am.* 59A.
- MENZER, G. (1928) Die Kristallstruktur der granate. *Zeit. Kristal.* **69**, 300-396.
- MIYASHIRO, A. (1953) Calcium-poor garnet in relation to metamorphism. *Geochim Cosmochim. Acta* **4**, 178-208.
- MROSE, M. E. AND D. E. APPLEMAN (1962) The crystal structure of väyrymenite and euclase. *Zeit. Kristal.* **117**, (1), 16-36.
- NEUNHAM, R. E. AND Y. M. DEHAAN (1962) Refinement of the $\alpha-Al_2O_3$, Ti_2O_3 , V_2O_5 and Cr_2O_3 structures. *Zeit. Kristal.* **117**, 235-237.
- PAULING, L. (1928) The principles determining the structure of complex ionic crystals. *Jour. Am. Chem. Soc.* **51**, 1010-1026.
- (1960) *The Nature of the Chemical Bond*. Third ed., Cornell University Press.
- PRANDL, W. (1964) Refinement of the garnet structure by neutron diffraction (abs.) *Solid State Comm.* **2**(1), 24.
- PRINCE, E. (1957) Neutron diffraction measurements on yttrium-iron and yttrium-aluminum garnets. *Acta. Cryst.* **10**, 787-788.

- SKINNER, B. J. (1956) Physical properties of end-members of the garnet group. *Am. Mineral.* **41**, 428-436.
- SMITH, J. V. AND S. W. BAILEY (1963) A second review of Al-O and Si-O tetrahedral distances. *Acta. Cryst.* **16**, 801-811.
- , I. KARLE, H. HAUPTMAN, AND J. KARLE (1960) The crystal structure of spurrite, $\text{Ca}_2(\text{SiO}_4)_2\text{CO}_3$. II. Description of structure. *Acta. Cryst.* **13**, 454-458.
- SUZUKI, T. (1960) Atomic scattering factor for O^{2-} . *Acta. Cryst.* **13**, 279.
- TRÖGER, E. (1959) Die Granatgruppe: beziehungen zwischen Mineralchemismus and Gesteinsart. *Neues Jahrb. Mineral.* **93**, 1-44.
- VAN DER HELM, D. (1961) Three and two dimensional Fourier summation program for crystal structure analysis with numerical and alphanumerical output. *1620 Programs I.C.R., Inst. Cancer Res., Philadelphia, Pa.*
- VERHOOGEN, J. (1958) Physical properties and bond type in Mg-Al oxides and silicates. *Am. Mineral.* **43**, 552-579.
- WEIDENBORNER, J. E. (1961) Least squares refinement of the structure of gadolinium-iron garnet, $\text{Gd}_3\text{Fe}_2\text{Fe}_3\text{O}_{12}$. *Acta. Cryst.* **14**, 1051-1056.
- ZEMANN, A. AND J. ZEMANN (1961) Verfeinerung der kristallstruktur von synthetischem pyrop, $\text{Mg}_3\text{Al}_2(\text{SiO}_4)_3$, *Acta. Cryst.* **14**, 835-837.
- ZEMANN, J. (1962) Zur Kristallchemie der Granate. *Beitr. Mineral. Petro.* **8**, 180-188.

Manuscript received, March 1, 1965; accepted for publication, July 28, 1965.